Polymer Film Dewetting by Water/Surfactant/Good-Solvent Mixtures: A Mechanistic Insight and Its Implications for the Conservation of Cultural Heritage

Michele Baglioni[+], Costanza Montis[+], David Chelazzi, Rodorico Giorgi, Debora Berti,* and Piero Baglioni*

Abstract: Aqueous nanostructured fluids (NSFs) have been proposed to remove polymer coatings from the surface of works of art; this process usually involves film dewetting. The NSF cleaning mechanism was studied using several techniques that were employed to obtain mechanistic insight on the interaction of a methacrylic/acrylic copolymer (Paraloid B72) film laid on glass surfaces and several NSFs, based on two solvents and two surfactants. The experimental results provide a detailed picture of the dewetting process. The gyration radius and the reduction of the T_g of Paraloid B72 fully swollen in the two solvents is larger for propylene carbonate than for methyl ethyl ketone, suggesting higher mobility of polymer chains for the former, while a nonionic alcohol ethoxylate surfactant was more effective than sodium dodecylsulfate in favoring the dewetting process. FTIR 2D imaging showed that the dewetting patterns observed on model samples are also present on polymer-coated mortar tiles when exposed to NSFs.

Aged and discolored varnishes, old fixatives, adhesives, and undesired paint layers are examples of filmogenic products that should be removed from the surfaces of paintings, sculptures, books, and other solid substrates. The removal of polymeric films from works of art is an important and delicate operation that might irreversibly damage the artifact,[1] especially when the cleaning is performed using organic solvents. Examples are the removal of coatings laid on porous substrates, such as wall paintings and stones,[2–4] or the selective removal of overpaintings from paintings or graffiti from street art.[5] In these contexts, neat organic solvents are poorly controllable, scarcely selective, and spread the dissolved material in the pores of the treated artifact.[1,6] Moreover, the use of solvents poses serious concerns about toxicity and eco-compatibility. Amphiphile-based nanostructured fluids (NSFs), such as micellar solutions and microemulsions, were proposed[7] to overcome these drawbacks. Several NSFs have been tested so far and their performances assessed both in laboratory and in real conservation tests for the removal of aged and discolored fixatives, or protective and consolidating agents from wall paintings.[3,4,8–13] Currently, several mechanistic aspects of the action of NSFs in polymer film removal are not fully understood. The comprehension of the mechanisms that rule the interaction between polymer coatings and nanofluids is indeed fundamental in this context. Works of art are highly complex and delicate systems and their cleaning must be fully controlled. By knowing in details the behavior of polymer films in the presence of cleaning fluids, that is, NSFs, it will be possible to tune their formulation and application technique so as to maximize their effectiveness or, even more importantly, to get maximum control on their cleaning action.

The interaction between NSFs and polymer thick films involves dewetting.[14] It is known that dewetting of thin polymer films (< 100 nm) can be induced by thermal annealing, exposure to vapors of the solvents, immersion in poor solvents, in water/solvent mixtures or, finally, in non-solvents.[15–20] We observed that the presence of amphiphiles in a water/good-solvent mixture can be key for dewetting thick polymer films from surfaces. This effect, practically unaddressed even in fundamental studies on thin films,[21,22] can be of paramount importance for applicative purposes in every field where dewetting is involved.

Recently,[23] dewetting was investigated for a NSF composed of water, propylene carbonate (PC) and a nonionic alcohol ethoxylate surfactant ($C_{9–11}E_6$) interacting with a p-(EMA/MA) 70:30 methacrylic/acrylic copolymer 5 μm thick film, commercially known as Paraloid B72. The presence of surfactant was key in promoting dewetting. Moreover, it has been shown that different surfactants, like $C_{9–11}E_6$ and sodium dodecylsulfate (SDS), in H_2O or H_2O/2-butanone (MEK) mixtures, produce different effects on polymeric coatings.[24,25]

Based on this state of the art, this contribution addresses two main issues: 1) the interactions with the polymer of NSFs containing two different solvents and two different surfactants was systematically investigated in a model system. In this way, that is, varying one component at a time, it was possible to isolate the role of each single chemical in the NSFs. The results clarify the specific role of solvents and surfactants in film dewetting, both from a thermodynamic and a kinetic standpoint; and 2) for the first time, the dewetting of thick polymer coatings was observed on samples representative of real conservation cases. This allowed transferring the model inferred from the observation on simplified systems to the cleaning of real works of art.

[*] Dr. M. Baglioni,[+] Dr. C. Montis,[+] Dr. D. Chelazzi, Prof. R. Giorgi, Prof. D. Berti, Prof. P. Baglioni
Department of Chemistry and CSGI, University of Florence
via della Lastruccia 3, 50019 Florence (Italy)
E-mail: debora.berti@unifi.it
baglioni@csgi.unifi.it

[+] These authors contributed equally to this work.

Supporting information and the ORCID identification number(s) for the author(s) of this article can be found under:
https://doi.org/10.1002/anie.201710930.
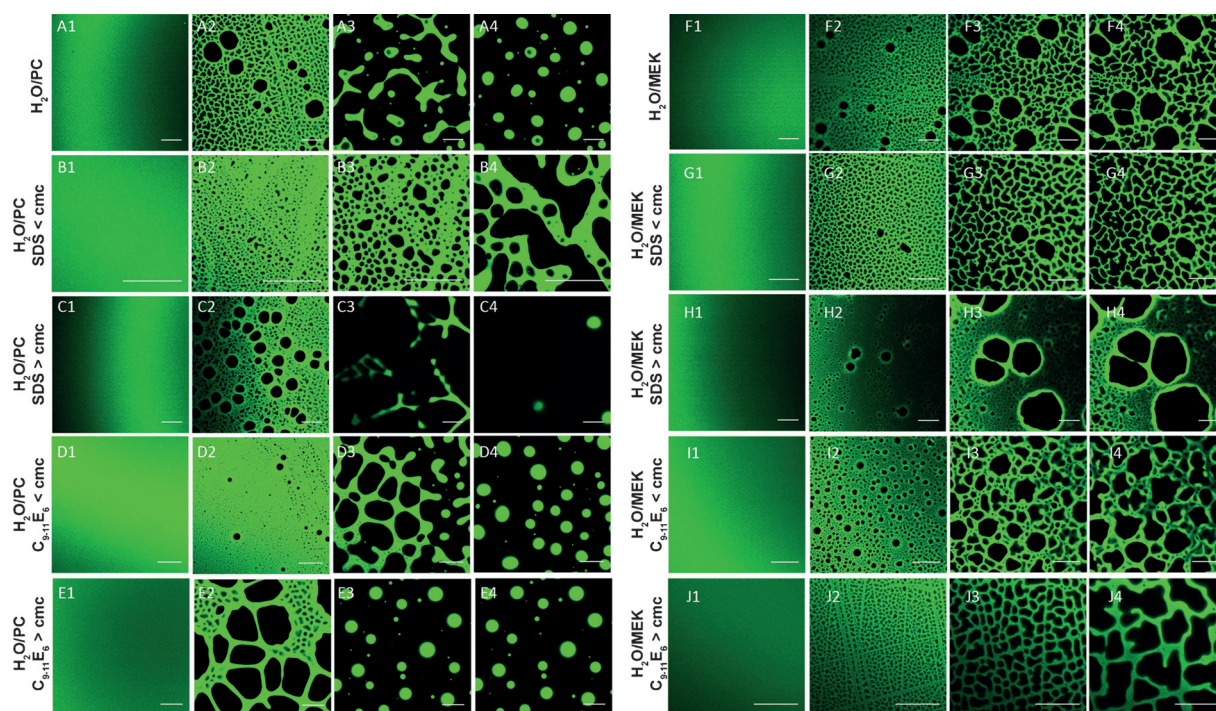
Figure 1. CLSM images of 1 µm-thick Paraloid B72 films containing coumarin 6 (green) monitored during 300 s (images 1 to 4 refer to $t=0$ s, $t=30$ s, $t=90$ s, $t=300$ s) of incubation with: A) H_2O/PC, B) H_2O/PC/SDS below cmc, C) H_2O/PC/SDS above cmc, D) H_2O/PC/$C_{9\text{-}11}E_6$ below cmc, E) H_2O/PC/$C_{9\text{-}11}E_6$ above cmc, F) H_2O/MEK, G) H_2O/MEK/SDS below cmc, H) H_2O/MEK/SDS above cmc, I) H_2O/MEK/$C_{9\text{-}11}E_6$ below cmc, and J) H_2O/MEK/$C_{9\text{-}11}E_6$ above cmc. Scale bars: 20 µm.

Figure 1 displays some representative confocal laser scanning microscopy (CLSM) images of horizontal sections of fluorescently-labeled 1 µm thick Paraloid B72 films laid on coverglasses, taken at the polymer/glass interface. With respect to other microscopic techniques, CLSM allows in situ imaging of different portions of the sample in a non-disruptive fashion and monitoring the interaction during its course at different heights. The morphology at the glass/polymer interface was followed for 5 min after addition of H_2O/MEK and H_2O/PC mixtures, without surfactants and with either $C_{9\text{-}11}E_6$ or SDS, below and above their critical micellar concentration (cmc; see the Supporting Information for detailed compositions and cmc). A complex and interesting picture emerges from CLSM images. The fluids interact with the film causing the local detachment of several regions (black areas, from $t=30$ s) of the film from the coverglass. These detachments slowly increase in size, and both their growth and film dewetting are highly dependent on the composition of the liquid phase. The systems containing PC are the most efficient, since they are able to dewet the polymer film also in the absence of surfactants (Figure 1 A). Conversely, only partial detachment is obtained with MEK-based fluids, which, however, have proved to promote complete dewetting for larger amounts of solvent in the NSF.[24] Interestingly, the surfactants differ in promoting the detachment and dewetting: $C_{9\text{-}11}E_6$ is faster and more efficient than SDS and it clearly accelerates dewetting with respect to bare solvent/H_2O mixtures (Figure 1 A3/E3 and F4/J4); on the other hand the contribution of SDS is clearly smaller and, for limited cases, slows down the process (Figure 1 A4/B4).

Finally, the efficiency of surfactants, in terms of polymer detachment and dewetting, is clearly boosted above the cmc (Figure 1 B3/C3, D3/E3, G4/H4, I4/J4).

To understand and rationalize this complex picture, the role of the solvent and of the surfactant have been separately addressed. According to their solubility parameters, both MEK and PC are considered good solvents for acrylic polymers,[26] but a systematic assessment of their affinity for Paraloid B72 has not yet been reported to the best of our knowledge. To this aim we performed small-angle neutron scattering (SANS) of 5 % w/w Paraloid B72 in the two deuterated solvents (Figure 2). The Flory theory predicts that the radius of gyration, R_g, scales with the chain length according to different power laws, depending on the solvent goodness. The same batch of Paraloid B72 has an average R_g of 3.5 nm in d-MEK and 5.0 nm in d-PC. The higher R_g in PC can be attributed to a higher solvation of the polymer coil, suggesting a higher affinity for this solvent, in agreement with CLSM observations. This is further confirmed by the reduction of T_g of Paraloid B72 fully swollen in the two solvents, which is larger for PC than for MEK (−22 °C and −20 °C respectively; DSC results in the Supporting Information). Therefore we can expect that at room temperature the mobility of the polymer chains will be higher for PC. These results can be safely extended to binary water/solvent mixtures, that is, the higher affinity of the solvent for the polymer represents a major driving force for dewetting.

Some of the differences observed for $C_{9\text{-}11}E_6$- and SDS-based NSFs in the presence of the same solvent deserve a more detailed analysis. One possible explanation concerns
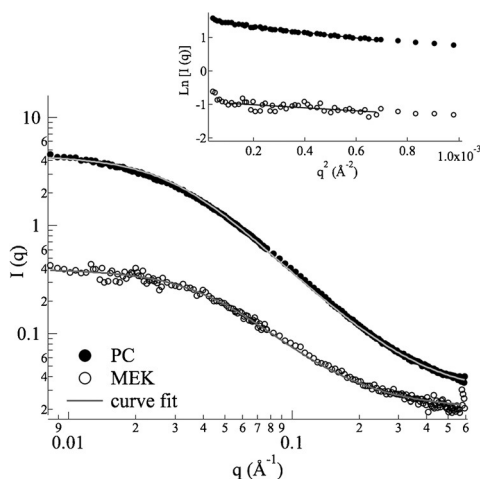
Figure 2. SANS curves of 5% w/w Paraloid B72 solutions in d-MEK (○) and d-PC (●) and fitting curves obtained according to a Gaussian chain model (——). Inset: Guinier plots.

different interaction of the surfactants with the solvents: surfactant assemblies can confine organic solvents and reduce their availability and their ability to swell the polymer film. However, this hypothesis was ruled out by investigating the nanostructure of the NSFs through small-angle X-ray scattering (SAXS) analyses (see the Supporting Information).

In fact, SAXS evidenced that only slight changes of micellar shape and size occur in the presence of MEK and PC, for both SDS and $C_{9-11}E_6$ dispersions above cmc. Owing to the relatively high solubility of both PC and MEK in water, the two solvents at the surfactant concentration employed in this study are mainly partitioned in the water medium ($>90\%$ and 75–80% for PC and MEK respectively, for both surfactants, according to SAXS fitting results), so that micelles in all the cases are in the binary water/solvent mixtures continuous phase.

The energetic balance of dewetting is described by the spreading coefficient, S, which, in the case of a polymer film laid on a glass surface and immersed in a liquid, can be expressed, within the Young formalism (see the Supporting Information), as a function of the surface tension of the liquid phase, γ_L, as follows [Eq. (1)]:

$$S(\gamma_L) = \gamma_L(\cos\theta_{LP} - \cos\theta_{LG}) + \gamma_p(\cos\theta_{PG} - 1) \quad (1)$$

where θ_{LP} is the contact angle of the liquid on the polymer surface in air, θ_{LG} is the contact angle of the liquid on glass in air, θ_{PG} the contact angle of the polymer on glass in air, and γ_P is the surface tension of the polymer in air.

When S is negative, dewetting is energetically favored and occurs spontaneously if an activation energy barrier is exceeded. To understand the precise role of the surfactant, we used Equation (1) to investigate the thermodynamic aspects.

Figure 3 (top) shows the surface tension of $C_{9-11}E_6$ and SDS in water. We notice that at the cmc the surface tension of the $C_{9-11}E_6$ solution is at least 10 mN m^{-1} lower than for SDS. Then, the contact angles, θ_{LG} and θ_{LG}, of H$_2$O, H$_2$O/$C_{9-11}E_6$ and H$_2$O/SDS solutions having different surface tensions
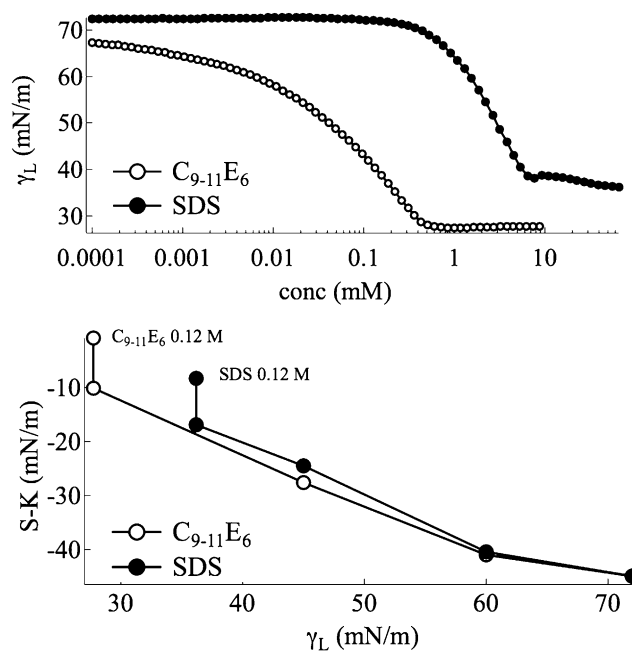
Figure 3. Top: Surface tension of $C_{9-11}E_6$ and SDS aqueous solutions as a function of surfactant molar concentration. Bottom: Trend of the spreading coefficient (S − K) as a function of γ_L, that is, the surface tension of the liquid phase for the case of a Paraloid B72 film laid on a glass surface and immersed in $C_{9-11}E_6$ and SDS water solutions. The points marked as $C_{9-11}E_6$ 0.12 M and SDS 0.12 M represent the calculation of S − K for surfactant mixtures having the actual concentration used in CLSM experiments for the systems above cmc. They have the same γ_L as the two points below, but, since the measured contact angles differ upon surfactant concentration, they are shifted towards higher values of S − K.

were measured on glass and on the Paraloid B72 film. The complete set of results is reported in the Supporting Information, Table S2. The measured values were used to calculate S for the two surfactants as a function of γ_L. The values γ_P and θ_{PG} are hardly measurable because the polymer is in a glassy state at room temperature, but they are invariant over the whole range of γ_L for the two binary water/surfactant mixtures, thus the whole second term in Equation (1) can be considered constant [Eq. (2)]:

$$\gamma_p(\cos\theta_{pG} - 1) = K \quad (2)$$

We can hypothesize that the contact angle θ_{PG} is slightly larger than 90° and that γ_P is around 40 mN m^{-1}, as reported in the literature for PMMA,[27] so that we can assume that $K \approx -40$ mN m^{-1}.

In Figure 3 (bottom), the trend of S − K as a function of γ_L is shown for the two surfactants. The trend is very similar for the two amphiphiles and, from an energetic standpoint, by increasing the concentration of surfactant, that is, by decreasing the surface tension γ_L, the film becomes less prone to dewet from glass, meaning that it is less unstable than in pure water. Moreover, the value of S − K for $C_{9-11}E_6$ 0.12 M in water is higher than the one for SDS 0.12 M, highlighting that, thermodynamically, $C_{9-11}E_6$ is more efficient than SDS in stabilizing the polymer film, so that dewetting is less favored.

We can thus conclude that the experimental results and dewetting cannot be fully accounted by a thermodynamic approach, and kinetic aspects are crucial. From this point of view, this implies that the surfactants have a role in lowering the energy barrier, which prevents the polymer from the thermodynamically favored dewetting. Furthermore, this also implies that the two surfactants have a different impact on the activation energy term: a different chemical affinity towards the polymer[25] might be at play, leading to a slow-down contribution of SDS, highlighted in few cases (Figure 1 B4); however, a more general effect of the surfactants is clearly relevant: as already discussed, the dewetting pathway involves the initial localized detachment of the polymer from glass (Figure 1), and the formation of new interfacial regions between the polymer–liquid, the polymer–solid, and solid–liquid interfaces, implying the formation of intermediate states where the overall interfacial area increases with respect to the initial intact film and to the final dewetted state.

A crucial role of the surfactant is in reducing the activation energy necessary to induce dewetting by decreasing the energy costs related to the formation of these intermediates, and the lower the interfacial tension the lower the energy barrier. From this standpoint, the surface activity of a surfactant is related to the reduction of surface tension at a defined concentration. Therefore the better performances of $C_{9-11}E_6$ over SDS can be explained by its higher surface activity (Figure 3, top). This hypothesis would also be consistent with the higher efficiency of both surfactants above their cmc in promoting dewetting with respect to the same systems below the cmc.

The overall NSF–polymer film interaction can be described from a kinetic standpoint as an interplay between the good solvent contribution in mobilizing the polymer chains (thus, the better the solvent, the more efficient is dewetting) and the surfactant contribution in lowering the interfacial energy of the dewetting intermediate states (thus, again, the better the surfactant, the more efficient is dewetting), all leading to the thermodynamically favored dewetted state, which is favored in all cases, but less unstable in the presence of a good surfactant.

These results represent a major advancement in understanding the removal mechanism operated by NSFs. Since we found that the effectiveness of the solvent and surfactant, respectively, in swelling the polymer film and lowering the interfacial tensions are key factors, we expect that these results can be safely extended to other NSFs that contain couples of good solvents/surfactants for given polymers. However, it must be noticed that all the experiments were carried out on simplified model samples constituted of relatively thin and homogeneous polymer films laid on glass slides.

In real conservation practice, thicker polymeric coatings are unevenly applied over rough and porous substrates, as for instance wall paintings. There are numerous case studies where NSFs proved effective at swelling and detaching layers of synthetic polymers from the surface of wall paintings. To verify if the polymer removal takes place via dewetting also for more representative surfaces, FTIR 2D imaging was used to investigate the removal of Paraloid B72 from mortar tiles.

The upward peak of the derivative absorption band at 1735 cm^{-1} (C=O stretching; see the Supporting Information) was used to map the presence of Paraloid B72 on mortar tiles that had been coated with the polymer, let dry for one week, and then immersed in the water/$C_{9-11}E_6$/PC system for 1 min, 3 min, and 5 min. The fluid was selected as it proved the most effective in dewetting the polymer from glass slides.

The visible light images and chemical maps of the surface of the tiles are shown in Figure 4. Immersion of the tiles in the fluid for 1 minute leads to the formation of craters of ca. 10–100 µm in the coating, where the polymer layer is thinned (green areas). Immersion for 3 minutes results in the for-
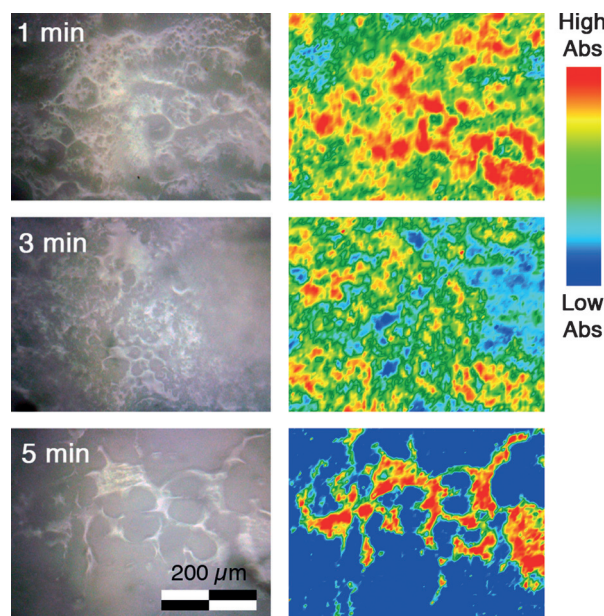
Figure 4. FTIR 2D imaging of mortar tiles coated with Paraloid B72 and immersed in the water/$C_{9-11}E_6$/PC system for 1 min, 3 min, and 5 min. Each row shows the image of the surface under VIS light (left) and the FTIR map of the polymer peak at 1735 cm^{-1} (C=O stretching; right). Scale bar: 200 µm. The spatial resolution of the chemical maps is 5.5 µm.

mation of holes of similar dimensions, which account for the initial steps of a dewetting process. The dimensions of craters and holes are similar to those observed on glass slides via CLSM. Immersion for 5 minutes leads to partial or to complete dewetting of Paraloid B72 from large portions of the surface (deep blue areas), leaving droplets and ripples of polymer. Different degrees of dewetting for the same immersion time account for the inhomogeneous thickness of the polymer layer. Overall, the observed dewetting pattern is very similar to that observed on glass slides, considering that both the polymer thickness and the type of substrate are significantly different in the two cases.

From an applicative standpoint, the induction of dewetting is of fundamental importance in the removal of polymer coatings from wall paintings. Firstly, the mere disruption of the film into separated polymer droplets is sufficient to partly recover the original physicochemical properties of the painting/air interface, reopening the porosity and letting the

painting transpire again. Secondly, the removal of the swollen polymer droplets is easily achieved by applying the NSF loaded in a cellulose poultice,[6] or using more advanced tools as chemical gels. The swollen polymer droplets stick to the poultice and are easily removed without any invasive mechanical action (that could be harmful to the paint layer). This methodology is particularly useful considering that works of art are often degraded, and exhibit fragile painted layers.

In conclusion, we found that the nature of solvent plays the most important role in the dewetting of polymer coatings on glass, that is, better solvents for the polymer are more efficient in swelling the film and inducing the mobility of polymer chains, needed to achieve dewetting. On the other hand, the surfactant nature is crucial to kinetically favor this process. The surfactant, lowering both the liquid/polymer and liquid/solid interfacial tensions, energetically favors the detachment of the film from the surface, which represents the first step of dewetting processes. Therefore, amphiphile-based systems having very low surface tension may be particularly effective in dewetting polymer films. Finally, the results of FTIR imaging on Paraloid B72-coated mortar tiles provide an explanation for the observed effectiveness of NSFs in real case studies, highlighting the mechanism through which they act and remove aged polymer coatings (cast from solutions). This opens to a series of investigations aimed at systematically refining specific cleaning fluids to target different types of coatings, with maximized effectiveness, control, and selectivity in the case of multilayered coatings.

Acknowledgements

Conflict of interest

The authors declare no conflict of interest.

[1] P. Baglioni, D. Chelazzi, *Nanoscience for the Conservation of Works of Art*, Royal Society Of Chemistry, London, **2013**.
[2] E. Carretti, L. Dei, *Prog. Org. Coat.* **2004**, *49*, 282–289.
[3] E. Carretti, L. Dei, C. Miliani, P. Baglioni, in *Trends Colloid Interface Sci. XV* (Ed.: P. P. G. Koutsoukos), Springer, Berlin, Heidelberg, **2001**, pp. 63–67.
[4] E. Carretti, R. Giorgi, D. Berti, P. Baglioni, *Langmuir* **2007**, *23*, 6396–6403.
[5] R. Giorgi, M. Baglioni, P. Baglioni, *Anal. Bioanal. Chem.* **2017**, *409*, 3707–3712.
[6] P. Baglioni, D. Chelazzi, R. Giorgi, *Nanotechnologies in the Conservation of Cultural Heritage: A Compendium of Materials and Techniques*, Springer, Berlin, **2014**.
[7] L. Borgioli, G. Caminati, G. Gabrielli, E. Ferroni, *J. Sci. Technol. Cult. Heritage* **1995**, *4*, 67–74.
[8] E. Carretti, L. Dei, P. Baglioni, *Langmuir* **2003**, *19*, 7867–7872.
[9] R. Giorgi, M. Baglioni, D. Berti, P. Baglioni, *Acc. Chem. Res.* **2010**, *43*, 695–704.
[10] M. Baglioni, R. Giorgi, D. Berti, P. Baglioni, *Nanoscale* **2012**, *4*, 42.
[11] M. Baglioni, Y. Jàidar Benavides, D. Berti, R. Giorgi, U. Keiderling, P. Baglioni, *J. Colloid Interface Sci.* **2015**, *440*, 204–210.
[12] M. Baglioni, M. Raudino, D. Berti, U. Keiderling, R. Bordes, K. Holmberg, P. Baglioni, *Soft Matter* **2014**, *10*, 6798–6809.
[13] M. Baglioni, Y. Jáidar Benavides, A. Desprat-Drapela, R. Giorgi, *J. Cult. Heritage* **2015**, *16*, 862–868.
[14] D. Gentili, G. Foschi, F. Valle, M. Cavallini, F. Biscarini, *Chem. Soc. Rev.* **2012**, *41*, 4430–4443.
[15] L. Xu, A. Sharma, S. W. Joo, *Macromolecules* **2012**, *45*, 6628–6633.
[16] L. Xu, T. Shi, L. An, *Langmuir* **2007**, *23*, 9282–9286.
[17] M. Cavallini, R. Lazzaroni, R. Zamboni, F. Biscarini, D. Timpel, F. Zerbetto, G. J. Clarkson, D. A. Leigh, *J. Phys. Chem. B* **2001**, *105*, 10826–10830.
[18] L. B. R. Castro, A. T. Almeida, D. F. S. Petri, *Langmuir* **2004**, *20*, 7610–7615.
[19] A. Verma, A. Sharma, *Macromolecules* **2011**, *44*, 4928–4935.
[20] H. J. Butt, K. Graf, M. Kappl, *Physics and Chemistry of Interfaces*, Wiley-VCH, Weinheim, **2003**.
[21] G. Reiter, R. Khanna, A. Sharma, *J. Phys. Condens. Matter* **2003**, *15*, S331.
[22] D. Fell, G. Auernhammer, E. Bonaccurso, C. Liu, R. Sokuler, H. J. Butt, *Langmuir* **2011**, *27*, 2112.
[23] M. Baglioni, C. Montis, F. Brandi, T. Guaragnone, I. Meazzini, P. Baglioni, D. Berti, *Phys. Chem. Chem. Phys.* **2017**, https://doi.org/10.1039/C7CP02608K.
[24] M. Raudino, G. Selvolini, C. Montis, M. Baglioni, M. Bonini, D. Berti, P. Baglioni, *ACS Appl. Mater. Interfaces* **2015**, *7*, 6244–6253.
[25] M. Raudino, N. Giamblanco, C. Montis, D. Berti, G. Marletta, P. Baglioni, *Langmuir* **2017**, *33*, 5675–5684.
[26] C. M. Hansen, *Hansen Solubility Parameters: A User's Handbook*, Second Edition, CRC Press, Boca Raton, FL, **2007**.
[27] L. A. Girifalco, R. J. Good, *J. Phys. Chem.* **1957**, *61*, 904–909.